Synthesis and Characterization of Fluorescent Polyoxometalate Nano-/Microrods

Yan Shen, Jun Peng, Changyun Chen, Dan Chen, Huanqiu Zhang, and Cuili Meng

Key Laboratory of Polyoxometalate Science of Ministry of Education, Faculty of Chemistry,
Northeast Normal University, Changchun, Jilin, 130024, People's Republic of China

Reprint requests to Prof. Dr. Jun Peng. Tel: +86-431-5099667. Fax: +86 4315099765.
E-mail: jpeng@nenu.edu.cn

Z. Naturforsch. **2010**, *65b,* 603 – 606; received December 29, 2009

Fluorescent nano-/microrods of the polyoxometalate (POM) $K_4H[Eu(\alpha\text{-}SiW_{11}O_{39})(H_2O)_2]\cdot 17H_2O$ were obtained in aqueous solution by a conventional synthesis method. The nano-/microrods have been characterized by elemental analysis and FT-IR, UV/Vis, and TG-DTA data, and their morphology was examined by ESEM-FEG, showing that the average ratio of diameter to length is 1 : 20. The obtained nano-/microrods exhibit a regular profile and an intense fluorescence.

Key words: Nano-/Microrods, Polyoxometalates, Photoluminescence Properties

Introduction

Polyoxometalates (POMs) are a distinct class of inorganic compounds with interesting structural versatility and unique redox properties, which have been employed in the areas of catalysis, medicine as well as a variety of functional materials [1 – 5]. POMs can accept electrons by undergoing stepwise multelectron redox processes, and their strong redox capability attracts considerable interest. Therefore, POMs can be considered as a kind of potential gasochromic and photochromic materials, which also can be used in constructing organic-inorganic hybrid luminescent materials.

Rare earth elements have long been known for their characteristic luminescence properties. Fluorescent materials of rare earths have many important practical applications, such as cathodoluminescent display phosphor screens, bioanalysis, electroluminescent optical devices, laser devices, and medical diagnosis [6 – 10], which have been fascinating researchers for decades. Rare earth-substituted POMs have been found to exhibit excellent luminescence properties [11, 12]. Especially the europium-containing polyanions have attracted attention, such as $[EuW_{10}O_{36}]^{9-}$ [13], $[Eu(SiW_{11}O_{39})_2]^{13-}$ [14], $[EuP_5W_{30}O_{110}]^{12-}$ [15], and $[Eu(\alpha\text{-}SiW_{11}O_{39})]^{5-}$ [16]. These polyanions have also been incorporated in various hybrid materials [17 – 19]. Mialane and coworkers systematically studied $\{Ln_x(SiW_{11}O_{39})\}^{8-3x}$ polyoxoanions, including $[Eu(\alpha\text{-}SiW_{11}O_{39})]^{5-}$ salts in which Na^+, K^+ and/or Cs^+ were counterions. Here we report on a simple method to obtain crystalline rods of $K_4H[Eu(\alpha\text{-}SiW_{11}O_{39})(H_2O)_2]\cdot 17H_2O$, and on their fluorescence properties.

Results and Discussion

Characterization of $K_4H[Eu(\alpha\text{-}SiW_{11}O_{39})(H_2O)_2]\cdot 17H_2O$ nano-/microrods

In the FT-IR spectrum of $K_4H[Eu(\alpha\text{-}SiW_{11}O_{39})(H_2O)_2]\cdot 17H_2O$, the absorption peaks at 1003 and

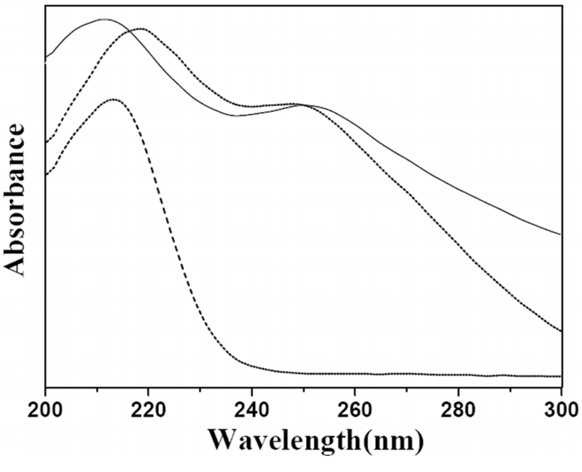

Fig. 1. UV/Vis spectra of $Eu(NO_3)_3$ (dashed line), $K_8[\alpha\text{-}SiW_{11}O_{39}]$ (dotted line) and $K_4H[Eu(\alpha\text{-}SiW_{11}O_{39})(H_2O)_2]\cdot 17H_2O$ (solid line).

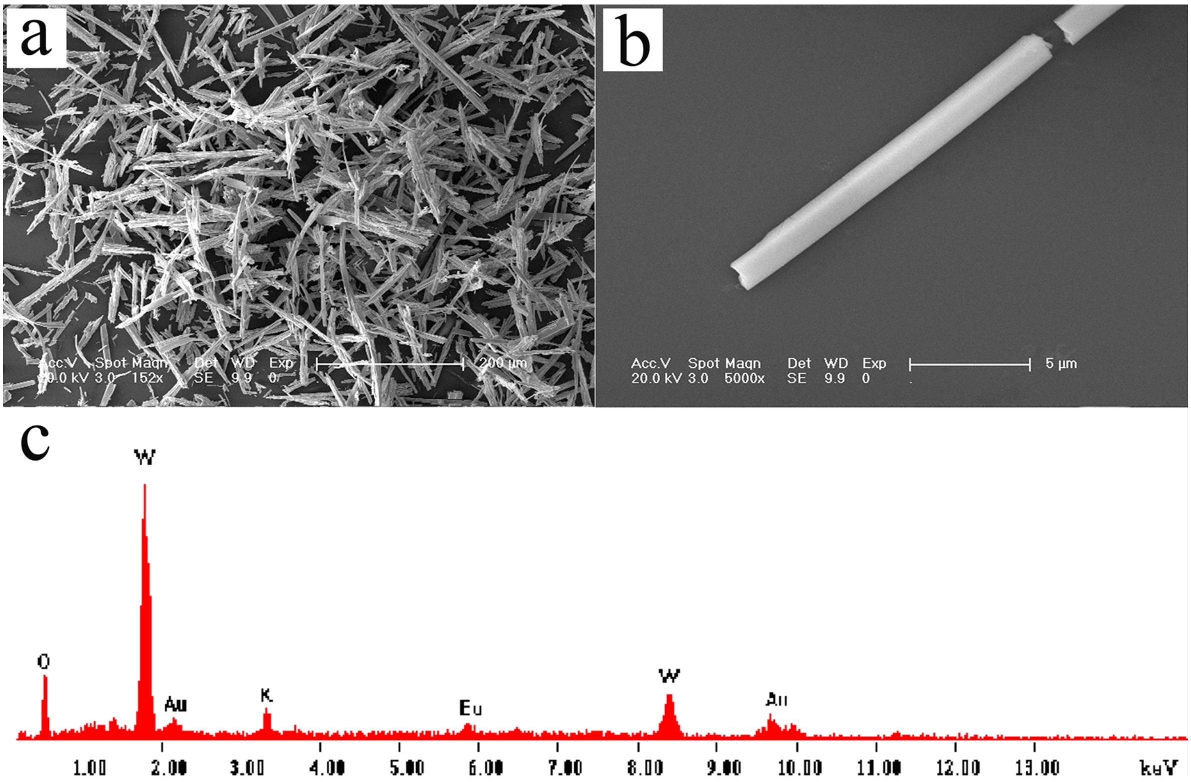

Fig. 2. ESEM-FEG images of $K_4H[Eu(\alpha\text{-}SiW_{11}O_{39})(H_2O)_2] \cdot 17H_2O$ nano-/microrods (a,b) and their EDS spectrum (c).

950 cm^{-1} correspond to metal-oxygen oscillations including Si–O and W=O stretching modes, respectively, and the absorption peaks between 900 and 600 cm^{-1} correspond to W–O–W stretching modes [20].

The UV/Vis spectrum of the fluorescent nano-/microrods of $K_4H[Eu(\alpha\text{-}SiW_{11}O_{39})(H_2O)_2] \cdot 17H_2O$ is represented in Fig. 1. The strong absorption peak around 210 nm is assigned to a $O_d \rightarrow W$ charge transfer transition, and the other absorption peak at 250 nm to a $O_{b,c} \rightarrow W$ charge transfer transition. These are the two characteristic bands of Keggin heteropolytungstates. However, the absorption peak at 210 nm has an obvious blue shift, and the intensity is enhanced compared to that of the raw material $K_8[\alpha\text{-}SiW_{11}O_{39}]$ (α-SiW_{11}), which confirms the combination of α-SiW_{11} and Eu^{3+}.

In the thermal decomposition process of $K_4H[Eu(\alpha\text{-}SiW_{11}O_{39})(H_2O)_2] \cdot 17H_2O$ nano-/microrods, the main mass loss of 9.1 % occurs below 150 ℃ with three distinct endothermic peaks at 61, 92 and 123 ℃ in the DTA plot corresponding to the loss of 17 water molecules [21]. In the temperature range of 150–400 ℃ the loss of 1.4 % corresponds to two water ligands bound to the Eu^{3+} center. Combined with TG-DTA data, the final formula of fluorescence nano-/microrods of POM is $K_4H[Eu(\alpha\text{-}SiW_{11}O_{39})(H_2O)_2] \cdot 17H_2O$.

The morphologies of the $K_4H[Eu(\alpha\text{-}SiW_{11}O_{39})(H_2O)_2] \cdot 17H_2O$ nano-/microrods, observed by ESEM-FEG, are shown in Fig. 2a. The crystalline clusters form rods with diameters of 300 nm to 3 μm, and the average ratio of diameter to length is 1 : 20. Fig. 2b shows an image of a single rod with smooth surface. The EDS spectrum (Fig. 2c) confirms the chemical composition of the $K_4H[Eu(\alpha\text{-}SiW_{11}O_{39})(H_2O)_2] \cdot 17H_2O$ nano-/microrods.

Photoluminescence properties of $K_4H[Eu(\alpha\text{-}SiW_{11}O_{39})(H_2O)_2] \cdot 17H_2O$ nano-/microrods

The excitation spectrum of the $K_4H[Eu(\alpha\text{-}SiW_{11}O_{39})(H_2O)_2] \cdot 17H_2O$ nano-/microrods measured at the emission wavelength of 614 nm shows the characteristic peaks of Eu^{3+} at 366 ($^7F_0 \rightarrow {}^5D_4$),

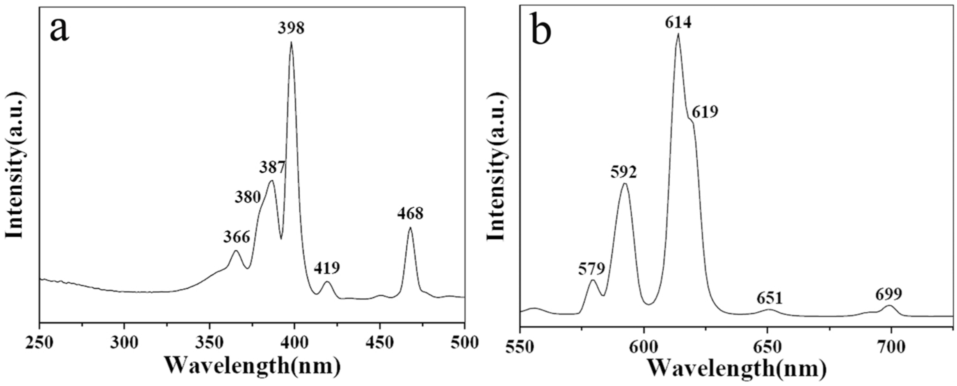

Fig. 3. Excitation spectrum (a) and emission spectrum (b) of $K_4H[Eu(\alpha\text{-}SiW_{11}O_{39})(H_2O)_2] \cdot 17H_2O$.

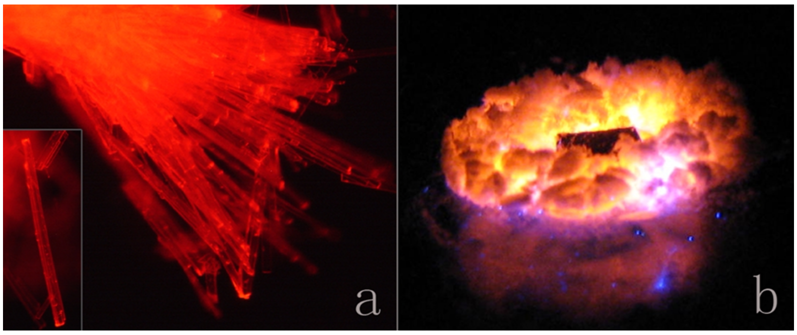

Fig. 4. Fluorescence microscopy images of $K_4H[Eu(\alpha\text{-}SiW_{11}O_{39})(H_2O)_2] \cdot 17H_2O$ nano-/microrods.

380 ($^7F_0 \rightarrow {}^5G_3$), 387 ($^7F_0 \rightarrow {}^5G_2$), 398 ($^7F_0 \rightarrow {}^5L_6$), 419 ($^7F_0 \rightarrow {}^5D_3$), and 468 nm ($^7F_0 \rightarrow {}^5D_2$) (Fig. 3a). The luminescence emission spectrum for the excitation at 398 nm is given in Fig. 3b. It shows five characteristic peaks of Eu^{3+} at 579, 592, 614, 651, and 699 nm, assigned to five transitions from the $^5D_0$ metastable state to the terminal levels ^7F_j ($j = 0, 1, 2, 3, 4$). The peak for the electronic dipolar transition $^5D_0 \rightarrow {}^7F_2$ is split into two peaks at 614 and 619 nm, and the intense secondary transition $^5D_0 \rightarrow {}^7F_1$ appears at 592 nm. The peak at 579 nm is ascribed to $^5D_0 \rightarrow {}^7F_0$, while the peaks at 651 and 699 nm correspond to $^5D_0 \rightarrow {}^7F_3$ and $^5D_0 \rightarrow {}^7F_4$ transitions, respectively [22–24].

Under UV excitation, the $K_4H[Eu(\alpha\text{-}SiW_{11}O_{39})(H_2O)_2] \cdot 17H_2O$ nano-/microrods show intense fluorescence. Fluorescence microscopy images of the $K_4H[Eu(\alpha\text{-}SiW_{11}O_{39})(H_2O)_2] \cdot 17H_2O$ nano-/microrods and the “Bird’s Nest” made of them are shown in Fig. 4.

Conclusion

Crystalline $K_4H[Eu(\alpha\text{-}SiW_{11}O_{39})(H_2O)_2] \cdot 17H_2O$ nano-/microrods have been obtained from aqueous solution by a simple method. They exhibit a regular profile and intense fluorescence, and thus may be used as potential one-dimensional fluorescent materials.

Experimental Section

Chemicals and measurements

Monolacunary tungstosilicate $K_8[\alpha\text{-}SiW_{11}O_{39}]$ (α-SiW_{11}) was synthesized according to the published procedure [25]. $Eu(NO_3)_3$ was prepared by dissolving the oxide in nitric acid. 732 Cation resin, Eu_2O_3, HNO_3, anhydrous ethanol and deionized water were purchased and used directly without any further purification. The FT-IR spectrum was recorded on a D/MAX-IIIC instrument, UV/Vis spectra on a 756 CRT spectrophotometer. TG-DTA was carried out on a Perkin-Elmer TGA7 instrument, ICP-AES on a Thermo iCAP 6000 inductively coupled plasma-atomic emission spectrometer, FL spectra on a Hitachi F-4500 photoluminescence spectrometer. ESEM-FEG images were acquired with an XL30 field-emission environmental scanning electron microscope after dispersing the samples in absolute alcohol with an ultrasonic vibrator. Fluorescence microscopy images were obtained on a Nikon Inverted Microscope TE2000 with a fluorescein isothiocyanate filter.

Preparation of $K_4H[Eu(\alpha\text{-}SiW_{11}O_{39})(H_2O)_2] \cdot 17H_2O$ *nano-/microrods*

3 g of α-SiW_{11} was dissolved in 10 mL deionized water, and the pH of the suspension was adjusted to 3 by adding cation exchange resin. Then the resin was filtered, and $Eu(NO_3)_3$ was added to reach pH = 1. The resulting solution was heated at 80 °C in a water bath for 15 min, then filtered and cooled to r. t. After one night the crystalline rods were harvested, washed with EtOH and dried in air. The chemical composition of the crystalline rods has been determined by ICP-AES. Anal. for $K_4H[Eu(\alpha\text{-}SiW_{11}O_{39})(H_2O)_2] \cdot 17H_2O$: calcd. Si 0.84, W 60.80, Eu 4.57, K 4.70; found Si 0.84, W 61.30, Eu 6.50, K 4.57.

Acknowledgement

We gratefully acknowledge the financial support by the Natural Science Foundation of China (20671016) and the Program for Changjiang Scholars and Innovative Research Team in University.

---

[1] T. Yamase, *Chem. Rev.* **1998**, *98*, 307 – 325.
[2] Z. F. Xin, J. Peng, T. Wang, B. Xue, Y. M. Kong, L. Li, E. B. Wang, *Inorg. Chem.* **2006**, *45*, 8856 – 8858.
[3] Y. H. Guo, Y. H. Wang, C. W. Hu, Y. H. Wang, E. B. Wang, *Chem. Mater.* **2000**, *12*, 3501 – 3508.
[4] A. Haimov, H. Cohen, R. Neumann, *J. Am. Chem. Soc.* **2004**, *126*, 11762 – 11763.
[5] D. A. Judd, J. H. Nettles, N. Nevins, J. P. Snyder, D. C. Liotta, J. Tang, J. Ermolieff, R. F. Schinazi, C. L. Hill, *J. Am. Chem. Soc.* **2001**, *123*, 886 – 897.
[6] V. Bekiari, P. Lianos, *Adv. Mater.* **1998**, *10*, 1455 – 1458.
[7] G. E. Buono-Core, H. Li, B. Marciniak, *Coord. Chem. Rev.* **1990**, *99*, 55 – 87.
[8] J. Kido, H. Hayase, K. Hongawa, K. Nagai, K. Okuyama, *Appl. Phys. Lett.* **1994**, *65*, 2124 – 2126.
[9] M. Li, P. R. Selvin, *J. Am. Chem. Soc.* **1995**, *117*, 8132 – 8138.
[10] F. S. Richardon, *Chem. Rev.* **1982**, *82*, 541 – 552.
[11] J. Wang, H. S. Wang, L. S. Fu, F. Y. Liu, H. J. Zhang, *Thin Solid Films* **2002**, *415*, 242 – 247.
[12] X. L. Wang, Y. H. Wang, C. W. Hu, E. B. Wang, *Mater. Lett.* **2002**, *56*, 305 – 311.
[13] R. D. Peacock, T. J. R. Weakley, *J. Chem. Soc. (A)* **1971**, *11*, 1836 – 1839.
[14] B. S. Bassil, M. H. Dickman, B. V. D. Kammer, U. Kortz, *Inorg. Chem.* **2007**, *46*, 2452 – 2458.
[15] I. Creaser, M. C. Heckel, R. J. Neitz, M. T. Pope, *Inorg. Chem.* **1993**, *32*, 1573 – 1578.
[16] P. Mialane, L. Lisnard, A. Mallard, J. Marrot, E. Antic-Fidancev, P. Aschehoug, D. Vivien, F. Sécheresse, *Inorg. Chem.* **2003**, *42*, 2102 – 2108.
[17] H. L. Li, W. Qi, W. L i, H. Sun, W. F. Bu, L. X. Wu, *Adv. Mater.* **2005**, *17*, 2688 – 2692.
[18] W. F. Bu, L. X. Wu, X. Zhang, A. C. Tang, *J. Phys. Chem. B* **2003**, *107*, 13425 – 13431.
[19] H. Y. Ma, J. Peng, B. B. Zhou, Z. G. Han, Y. H. Feng, *Appl. Surf. Sci.* **2004**, *233*, 14 – 19.
[20] S. Lis, *J. Alloys. Compd.* **2000**, *300 – 301*, 88 – 94.
[21] Z. Wang, J. Wang, H. J. Zhang, *Mater. Chem. Phys.* **2004**, *87*, 44 – 48.
[22] J. Wang, H. S. Wang, L. S. Fu, F. Y. Liu, H. J. Zhang, *Thin Solid Films* **2002**, *414*, 256 – 261.
[23] J. Wang, Z. Wang, H. S. Wang, F. Y. Liu, L. S. Fu, H. J. Zhang, *J. Alloys. Compd.* **2004**, *376*, 68 – 72.
[24] J. Wang, H. S. Wang, F. Y. Liu, L. S. Fu, H. J. Zhang, *J. Lumin.* **2003**, *101*, 63 – 70.
[25] A. Tézé, G. Hervé, *J. Inorg. Nucl. Chem.* **1977**, *39*, 999 – 1002.